Materials Science & Engineering A 690 (2017) 348–354

Contents lists available at ScienceDirect

Materials Science & Engineering A

journal homepage: www.elsevier.com/locate/msea

A deformation-processed Al-matrix/Ca-nanofilamentary composite with low density, high strength, and high conductivity

Liang Tian[a,*], Alan Russell[b,c], Trevor Riedemann[c], Soeren Mueller[d], Iver Anderson[b,c]

[a] Department of Materials Science and Engineering, University of Michigan, Ann Arbor, MI 48109, USA
[b] Department of Materials Science and Engineering, Iowa State University, Ames, IA 50011, USA
[c] Ames Laboratory of the US Department of Energy, Ames, IA 50011, USA
[d] Technische Universität Berlin, Gustav-Meyer-Allee 25, 13355 Berlin, Germany

ARTICLE INFO

Keywords:
Metal matrix composite (MMCs)
Powder processing
Severe plastic deformation
Strength
Electrical resistivity/conductivity

ABSTRACT

Light, strong materials with high conductivity are desired for many applications such as power transmission conductors, fly-by-wire systems, and downhole power feeds. However, it is difficult to obtain both high strength and high conductivity simultaneously in a material. In this study, an Al/Ca (20 vol%) nanofilamentary metal-metal composite was produced by powder metallurgy and severe plastic deformation. Fine Ca metal powders (~200 μm) were produced by centrifugal atomization, mixed with pure Al powder, and deformed by warm extrusion, swaging, and wire drawing to a true strain of 12.9. The Ca powder particles became fine Ca nanofilaments that reinforce the composite substantially by interface strengthening. The conductivity of the composite is slightly lower than the rule-of-mixtures prediction due to minor quantities of impurity inclusions. The elevated temperature performance of this composite was also evaluated by differential scanning calorimetry and resistivity measurements.

1. Introduction

Low density, high strength, and high electrical conductivity are desirable material properties for many applications such as electric power transmission cables, fly-by-wire control systems, and downhole power feeds [1]. However, it is challenging to produce a material with both high strength and high electrical conductivity. Conventional strengthening methods such as strain hardening, second-phase hardening, precipitate hardening, or solid solution hardening significantly decrease conductivity. A type of composite called deformation processed metal-metal composites (DMMCs) has been found to exceed the rule-of-mixtures strength prediction and also deliver an electrical conductivity nearly equal to the rule-of-mixtures prediction [2]. DMMCs are produced by (1) powder metallurgy or (2) solidification of a liquid solution of two elements that are mutually insoluble in the solid state, followed by severe plastic deformation [3]. The two metal phases used for composite production must be highly ductile to sustain deformation true strain as high as 16 without fracturing. The second (minority) phase deforms into fine filaments that reinforce the composite by interface strengthening, which strengthen the metal by blocking dislocation glide at the interfaces. DMMCs are essentially nano-scale bundles of two pure metals whose unique microstructure provides minimal electron scattering effect (along the filament direction) from solute impurities, interfaces, grain boundaries, or dislocations [4].

Though many DMMC systems have been studied in the past few decades [2], none possess densities and electrical conductivities close to those of pure Al. Al/Ca DMMCs were invented [5] to produce a light, highly conductive, high-strength composite conductor. Both Al and Ca are low-density, low-cost, and highly ductile fcc metals. They are the fourth and fifth most conductive metallic elements (after the three Group 11 elements: Cu, Ag, and Au). In Al/Ca DMMCs, the highly reactive Ca filaments are embedded inside the Al matrix, which isolates the Ca from environmental oxygen and moisture, giving the composite excellent corrosion resistance. The first-generation Al/Ca (9 vol%) composite was produced to prove this concept and to study the microstructure-property relationships [6]. However, the Ca metal used in producing that first-generation composite was commercially available Ca granules with average diameter around 1.2 mm. After a deformation true strain of 13.7, these granules were deformed into 2 μm filaments, which were still too coarse to provide the large strength increases seen in previous investigations on Al/Mg [7] and Al/Ti [8]. The investigations on Al/Mg and Al/Ti DMMCs demonstrated low densities and high strengths, but Mg's conductivity is mediocre and Ti's is poor, rendering unexceptional conductivities.

* Corresponding author.
E-mail address: lilangt@umich.edu (L. Tian).

http://dx.doi.org/10.1016/j.msea.2017.03.010
Received 24 November 2016; Received in revised form 2 March 2017; Accepted 3 March 2017
Available online 06 March 2017

In this study, we used Ca metal powders with average diameter around 200 μm to produce second-generation composite, Al/Ca (20 vol %). It was anticipated that the finer Ca filaments and larger Ca volume fraction would produce higher strength. Since no commercial vendors produce fine Ca metal powders, Ca powders used in this experiment were produced by a centrifugal atomization device designed and fabricated at the Ames Laboratory of the U.S D.O.E [9]. The processing, microstructure, and strength/conductivity relationship in Al/Ca (20 vol %) composite were studied, and the results are reported here.

2. Experimental procedure

High-purity (99.99%) Al powders produced by the Ames Laboratory gas atomization reaction synthesis (GARS) process (45–106 μm) were mixed with high-purity (99.5%) fine Ca metal powder (106–212 μm) produced by the aforementioned centrifugal atomization system [10]. Mixed powders (80 vol%, 157 g Al and 20 vol%, 22.4 g Ca) were die pressed into cylindrical powder compacts (diameter 75 mm, height 25.4 mm) under a pressure of 40.6 MPa. The powder compacts had a density of 65%, which matched the compressibility curve for gas atomized Al powder [11]. The powder compacts were loaded into a pure Al (1100-H14) extrusion can (inside diameter 78 mm, outside diameter 90 mm and internal length 196.8 mm) and outgassed *in vacuo* at a pressure of 2.7×10^{-5} Pa to remove gasses and moisture adsorbed on the powder particles, prior to e-beam welding the container's end cap. The extrusion can loaded with Al/Ca powder compacts were extruded at the Extrusion Research & Development Center at the Technical University of Berlin, Germany, to produce Al/Ca (20 vol%) composite rod. The indirect extrusions were done using a container with an inner diameter of 95 mm and an extrusion die with a die orifice of 27.3 mm. For the billets, an initial temperature of 285 °C was chosen, which was thought to be hot enough to activate a sufficient number of slip systems to promote easy deformation but cool enough to avoid formation of Al-Ca intermetallics. Extrusion was done with an extrusion force of 1.9 MN in the stationary condition at a ram speed of 1.5 mm/s. The metal billet diameter reduced from 89 mm to 27.3 mm, which gives an extrusion ratio of 10.6. The deformation true strain η of the specimen is calculated by $\eta=2\mathrm{In}(d_0/d_f)$, where d_0 and d_f are the initial and final specimen diameters, respectively. The as-extruded composite specimen had a deformation true strain of 1.93, after accounting for its 35% porosity and void space in the container. The extrusion process transforms spherical Ca metal particles into co-axial filaments.

The Al sleeve from the pure Al extrusion can was removed from the Al/Ca composite rod with a lathe. Further deformation at room temperature by swaging was conducted. The composite rod was reduced to 2.95 mm diameter wire (deformation true strain 6.39). The middle section of the 2.95 mm composite wire was further swaged at room temperature to 1 mm diameter (deformation true strain 8.52). Wire drawing was used from this point to achieve a deformation true strain of 12.9 and wire diameter of 0.112 mm. At a true strain of 12.9, the Al/Ca composite was expected to contain Ca filaments with average diameter around 200 nm, which should be sufficiently fine to induce a substantial strengthening effect, while maintaining high electrical conductivity [4].

Microstructure, tensile strength, and electrical conductivity were measured at various deformation true strain levels. Microstructures were studied by field emission-scanning electron microscopy with a Quanta 250 instrument. Lower true-strain specimens were prepared for metallography by polishing on SiC grinding paper with hexane to 1200 grit; further polishing was performed using 1 μm glycol-diamond polishing fluid. (Conventional polishing fluids like MetaDi or organic solvents cannot be used because they contain trace amounts of water that attack the Ca filaments.) Focused-ion-beam cutting followed directly by SEM imaging was employed for the η=12.9 sample to eliminate polishing and exposure to air.

Tensile tests were done with an Instron 3367 system using an elongation rate of 2 mm/min. (average of three independent tests) of the Al/Ca (20 vol%) sample at true strain levels lower than 8.5. A Zwick/Roell Model Z 2.5 tensile tester was used for testing samples with deformation true strains 8.5 and above; while the η=12.9 samples were measured at Psylotech's facility on their μTS, an “under-microscope” universal test system. Sample length was measured between grip fronts with a caliper. Specimen diameter was measured using pixel measurement from the 5×2 optics of the microscope. An average of several diameter data points along the length of the sample was used for the area calculation. The elongation ramp rate is about 240 μm/s.

Differential scanning calorimetry (DSC) tests were conducted on a Netzsch STA449 F1 DSC system with a heating rate of 5 °C/min on Al/Ca samples with various deformation true strain levels to evaluate the microstructure evolution at elevated temperature.

Electrical resistivity/conductivity data were measured by the four-point probe method with a Keithley 224 constant current source (100 mA) and a Keithley 614 electrometer for both as-deformed and annealed 1 mm Al/Ca wire samples to study the effects of annealing time and temperature on the microstructure. Similar processing procedures of Al/Ca wire were performed on pure Al powders of the same size range to get pure Al powder compacts (64% dense) to be deformed into 1 mm pure Al wire (deformation true strain 8.52), which serve as a control specimen in resistivity measurements.

3. Results and discussions

3.1. Microstructure characterization of Al/Ca (20 vol%) composite

Fig. 1 shows the as-deformed microstructure of Al/Ca (20 vol%) composite at different deformation true strains. The light gray Ca filaments adopted a ribbon-shaped morphology instead of the expected cylindrical shape. According to the classic composite morphology theory [2,12], in a fcc matrix DMMC, a bcc metal filament tends to develop a < 110 > fiber texture parallel to the deformation axis, which leads to a plain strain deformation mode that would form a ribbon-like curling filamentary morphology. In contrast, fcc filaments tend to deform axi-symmetrically to develop a cylindrical filament morphology due to the larger number of slip planes available in a textured fcc matrix.

It is possible that the ribbon-shaped Ca filaments, apparent in Fig. 1(b) and (c), result from the temporary temperature rise and large shear stress present during extrusion, causing a temporary crystal structure transformation from fcc Ca to bcc Ca. It should be noted that the equilibrium fcc-bcc transformation in pure Ca occurs at 728 K [13].

The Ca filament thickness can be measured from the SEM micrographs, and are summarized in Table 1. It is readily apparent that the filament thickness decreased sharply as deformation true strain increased. An exponential dependence of filament thickness on deformation true strain was found to be $120.3\exp(-0.499\eta)$ (μm). This thickness dependence matched well with the ideal Hall-Petch thickness dependence $d_0\exp(-0.5\eta)$ (μm), where d_0 is between 100 and 200 μm.

3.2. Strength of Al/Ca (20 vol%) composite

Fig. 2 shows the tensile testing stress-strain curves for Al/Ca tensile specimens at various deformation true strains. The tensile strengths at various deformation true strain levels are summarized in Table 2.

Fig. 3 shows the experimental relationship between deformation true strain and tensile strength of Al/Ca composite wires and the fitting result by a Hall-Petch barrier model, which gave the strength as $81.53+157.2/\mathrm{sqrt}[120.3\exp(-0.499\eta)]$ MPa. As these data show, as the deformation true strain increases, the tensile strength increases exponentially for this Al/Ca (20 vol%) composite. This suggests that the strengthening effect of Al/Ca composite is largely contributed by

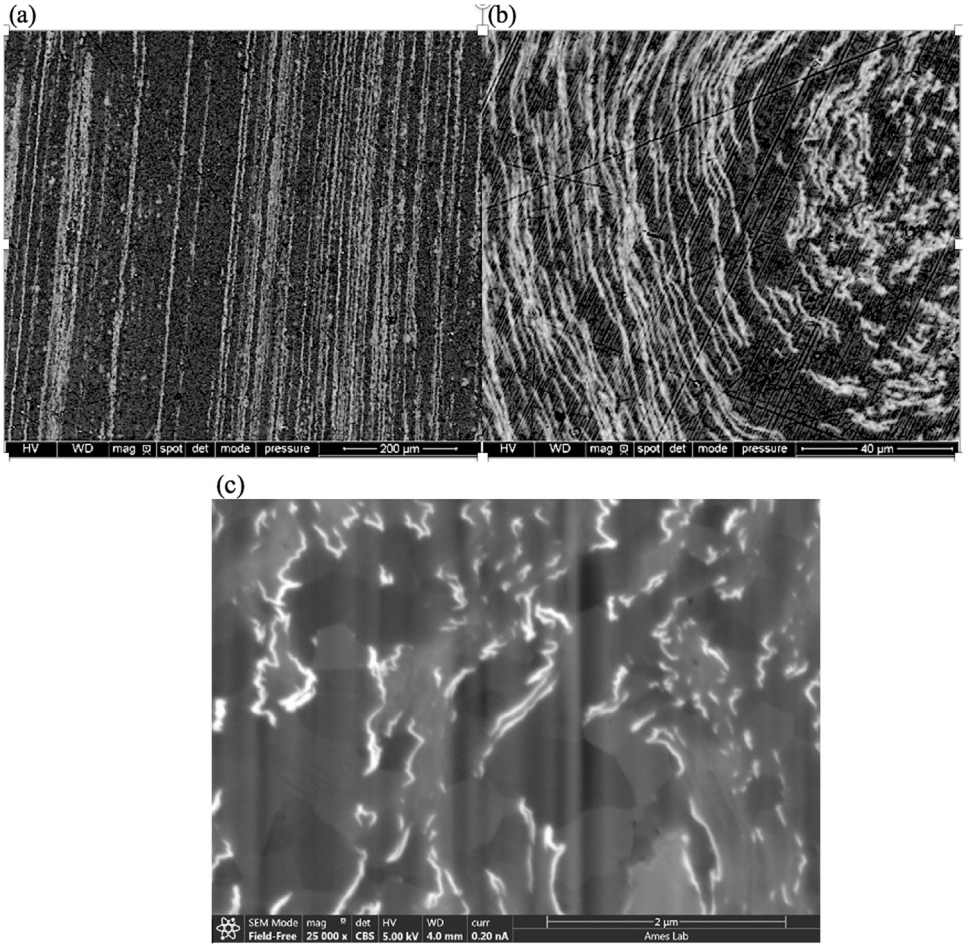

Fig. 1. Back-scattered electron SEM (scanning electron microscopy) micrographs of Al-Ca (20 vol%) composite: (a) longitudinal cross section at deformation true strain η 6.38, (b) transverse cross section at η 8.52, (c) transverse cross section at η 12.91. The light-gray phase is Ca; the dark-gray phase is Al. Grain structure contrast is visible within the Al in (c). The vertical bands in this micrograph are "curtaining" artifacts from the focused-ion beam cutting.

Table 1
Calcium filament thicknesses at different deformation true strains measured from the SEM micrographs in Fig. 1.

Deformation true strain η	Ca filament thickness (μm)
6.38	4.97
8.52	1.76
12.91	0.05

interface strengthening that is much less effective at low deformation true strain levels due to the small interface area associated with the coarse Ca filament size. The interface area increases exponentially with increasing deformation true strain due to the smaller Ca filament size. At high deformation true strains, the Ca filament thickness was reduced to the submicron regime (Fig. 1c), which generates a large amount of interface area to strengthen the composite by acting as barriers to dislocation motion [3].

Fracture surface of tensile tested sample at deformation true strain 12.9 are exhibited in Fig. 4. The fracture surface shows the feature of ductile fracture mode. The fracture surface of tensile tested samples at lower deformation true strain shows similar features. This suggests that the Al/Ca composite wire possesses some ductility even at this high true strain level of deformation processing.

3.3. Differential scanning calorimetry measurements on Al/Ca (20 vol%) composite

Differential scanning calorimetry (DSC) tests were performed in Ar atmosphere on Al/Ca (20 vol%) composite to explore possible microstructure transformations at elevated temperature. Previous investigation on Al/Ca (9 vol%) composite [6] suggested that there are two exothermic reactions occurring during DSC testing. One is the formation of Al_4Ca at 225 °C and the other is the formation of Al_2Ca at 275 °C [6]. The formation of these intermetallic compounds would alter the performance of the Al/Ca composite conductor at the mildly elevated temperatures that occur during routine conductor service and the substantially elevated temperatures that can occur during emergency overloading. Formation of the intermetallics is irreversible, and they persist even when the metal is subsequently cooled to room temperature. Therefore, studying these reactions for Al/Ca (20 vol%) composite at elevated temperature is important. Fig. 5 shows the DSC curves for various Al/Ca (20 vol%) composite samples at different deformation true strains. It is clear that intermetallic formation begins at a higher temperature for as-extruded samples with low deformation true strain than for samples deformed to high true strain. This is probably attributable to the fact that the micron- and submicron-size Ca filaments in highly deformed samples possess a greater driving force for the reaction due to curvature-driven atomic mixing from the Gibbs-Thompson effect [14]. Also, in the as-extruded (η=1.93) sample, there

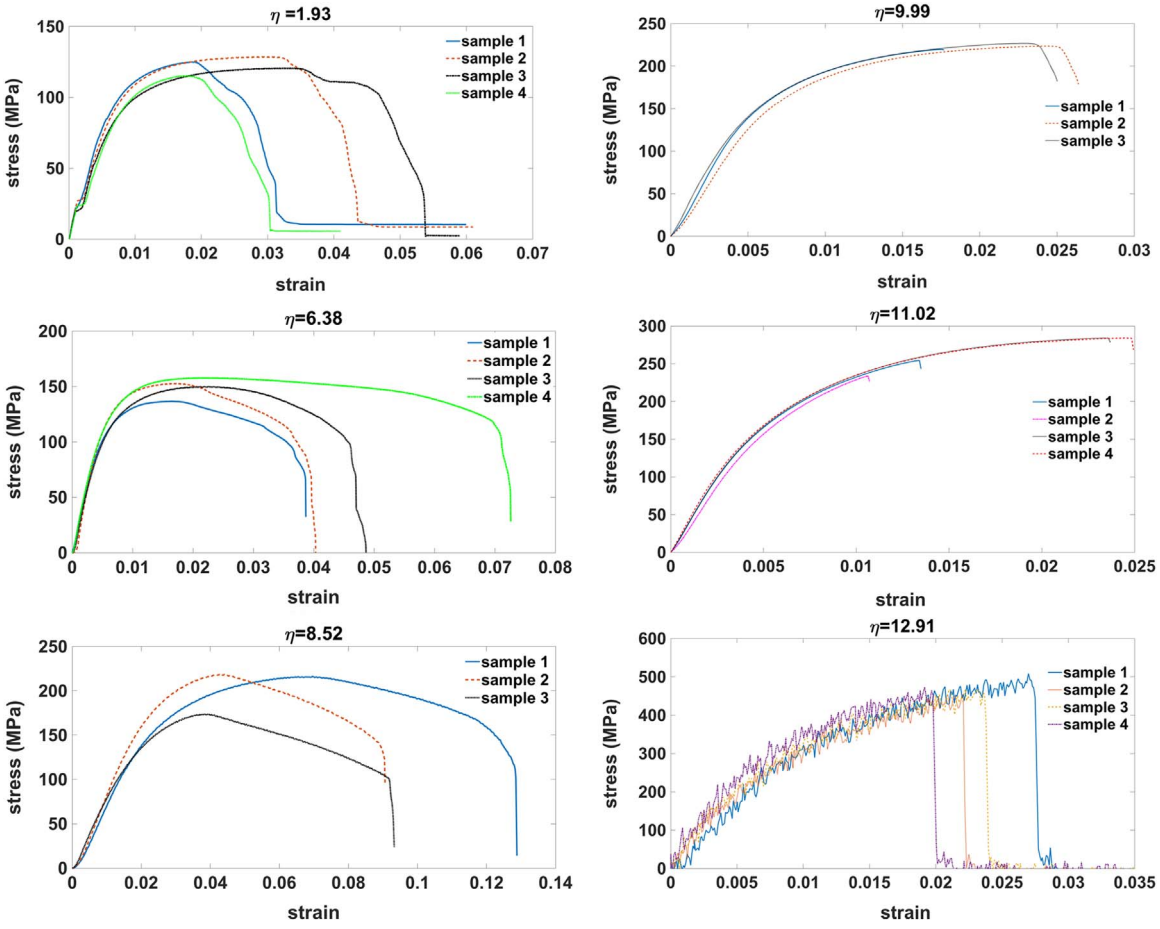

Fig. 2. Tensile tests of Al/Ca (20 vol%) composite at various deformation true strain levels.

Table 2
The ultimate tensile strength of Al/Ca (20 vol%) composites at various deformation true strains.

Deformation true strain	Ultimate tensile strength (MPa)
1.93	122
6.38	168
8.52	206
9.987	223
11.02	264
12.91	476

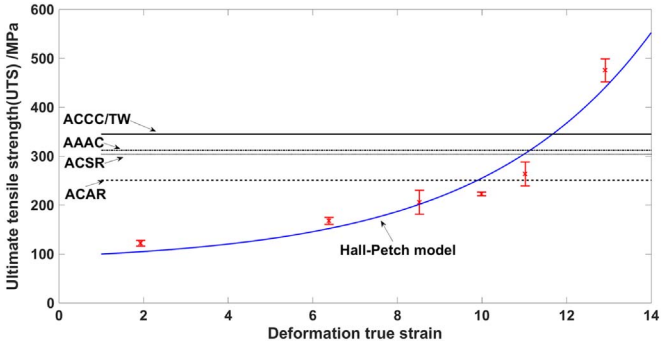

Fig. 3. Tensile strength of Al-20 vol%Ca composite as a function of deformation true strain. The experimental data are fitted by a Hall-Petch barrier model, which is the solid curve. The ultimate strengths of four commonly used commercial conductors are shown for comparison. (ACAR=Aluminum Conductor Aluminum Alloy Reinforced; ACSR=Aluminum Conductor Steel Reinforced; AAAC=All Aluminum Alloy Conductor; ACCC/TW=Aluminum Conductor Composite Core with Trapezoidal Wire cross section.).

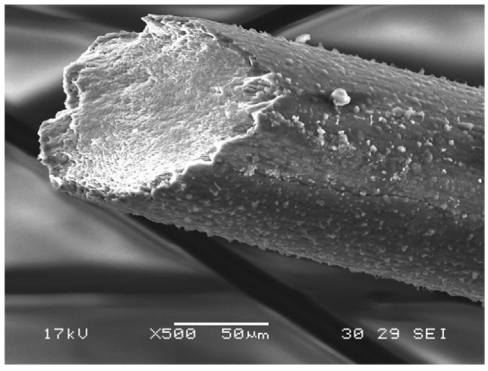

Fig. 4. The fracture surface of tensile tested sample at deformation true strain of 12.9.

appears to be one exotherm with an onset temperature of 335.4 °C. In contrast, in the two as-swaged samples (η=6.38 and 8.52), two exothermic events have been observed. The first event is presumably due to the Al_4Ca formation, since the Al_4Ca formation has a less negative enthalpy of formation [ΔH_f (Al_4Ca, solid, 298 K)=−43.9 ± 4.2 kJ/mol] than that of Al_2Ca [ΔH_f (Al_2Ca, solid, 298 K)=−73.2 ± 4.2 kJ/mol] [15], which causes the first exothermic peak to be small. The binary phase diagram for the Al-Ca system is shown in Fig. 6 for reference. In addition, Al_4Ca is less stable [ΔG_f (Al_4Ca, solid, 800 K) =−17800 ± 140 J/mol] and will decompose into Al_2Ca [ΔG_f (Al_2Ca, solid, 800 K)=−28500 ± 300 J/mol]. The second event presumably results from the formation of Al_2Ca, which is the most stable

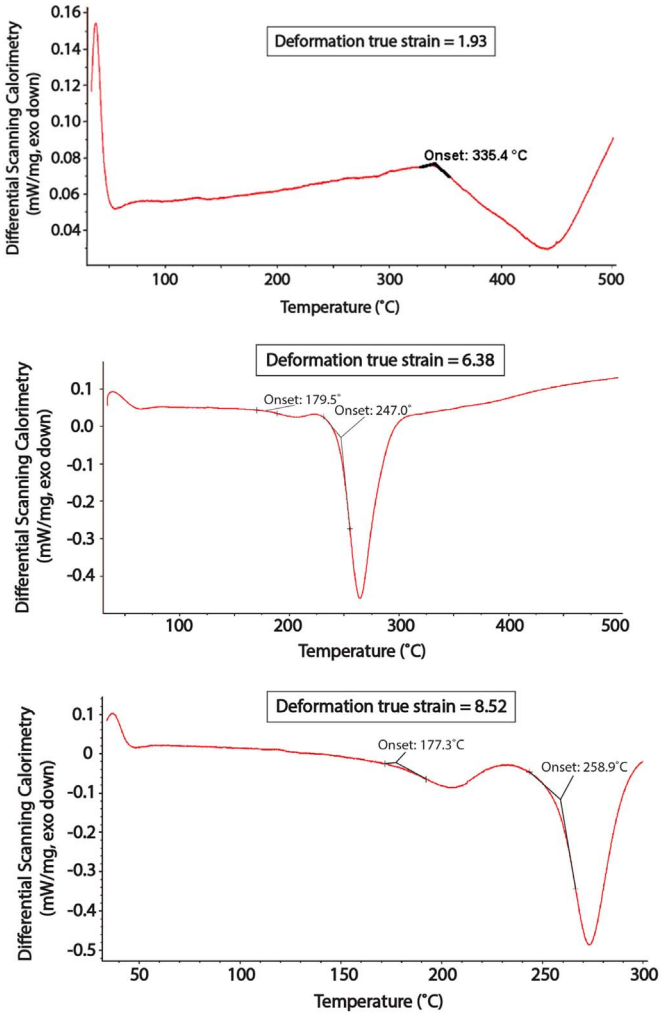

Fig. 5. The DSC curves for Al/Ca (20 vol%) composite samples at different deformation true strains under argon atmosphere. The as-extruded 27.3 mm sample has deformation true strain of 1.93. The as-swaged 3 mm sample has deformation true strain 6.38. The as-swaged 1 mm sample has deformation true strain 8.52.

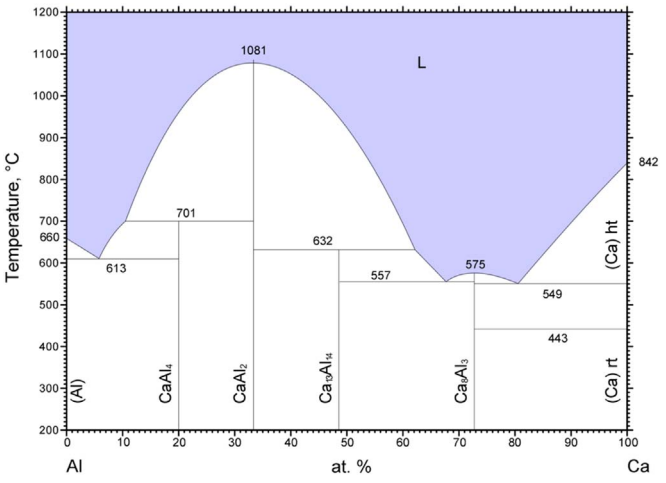

Fig. 6. Phase diagram for the Al-Ca system. ASM Diagram no. 1600365, Okamoto (2003) [13].

intermetallic compound in the Al-Ca binary system with a melting temperature of 1081 °C, as seen in Fig. 6.

3.4. Electrical resistivity of Al/Ca (20 vol%) composite and pure Al

The electrical resistivity of as-deformed 1 mm Al/Ca composite wire and 1 mm pure Al wire (deformation true strain=8.52) were determined by four-point probe resistivity measurement. The electrical resistivity of 1 mm Al/Ca (20 vol%) composite wire was measured to be 0.0305 μΩ m, while the measured resistivity of 1 mm pure Al wire was 0.0283 μΩ m. The resistivity of the composite is 3.4% higher than the predicted 0.0295 μΩ m by the inverse rule of mixtures. This difference may result from crystal defects such as powder particle oxide layer debris inclusions and/or from an increased dislocation density. Increased dislocations could be from statistically stored dislocations (SSDs) and/or geometrically necessary dislocations (GNDs), both of which result from the strain hardening and increased interface area. Since the pure Al specimen was observed to dynamically recrystallize during deformation, the resistivity measurements on annealed pure Al wire suggest that the resistivity originating from increased dislocation density by strain hardening is negligible. In the Al/Ca composite wire, the GNDs are generated to accommodate the Al/Ca interface area, which could be another contribution to resistivity when the Ca filaments are submicron in size. However, in the 1 mm Al/Ca composite wire, the Ca filament size is close to 2 μm, which is too coarse to generate a strong interface scattering effect. It is also possible that the elevated resistivity values for Al/Ca composite wires result from deformation-induced chemical mixing to form localized solid solutions that increase the resistivity.

The resistivity of Al/Ca (20 vol%) composite at deformation true strain 12.9 was predicted by the model proposed in Ref. [4]. The mean free path of Al and Ca was estimated to be 14 and 27 nm according to Ref [16]. From the microstructure image of composite wire with deformation true strain 12.9 shown in Fig. 1, the average Ca ribbon shaped filament thickness is about 50 nm and the average Al matrix phase thickness (filament spacing) is about 500 nm. Based on Ref. [4] Eq. (2) for ribbon shaped filaments and Eq. (4) for matrix, the modified Al matrix resistivity and Ca filament resistivity considering the interface scattering is 0.0286 μΩ m and 0.0396 μΩ m with a reasonable estimating choice of p=0.5. The resistivity of Al/Ca (20 vol%) composite at deformation true strain 12.9 is predicted to be 0.0303 μΩ m by modified inverse rule of mixtures. The conductivity 33.02 $(\mu\Omega\ m)^{-1}$ is higher than most current commonly used conductors in Ref [1].

The electrical resistivity values of the Al/Ca composite wire and pure Al wire annealed at elevated temperature have been measured to evaluate the effect of possible high-temperature annealing in electrical transmission service that may alter both the microstructure and the resistivity of Al/Ca composite wire. Tables 3 and 4 present the resistivity of 1 mm Al/Ca composite wire and 1 mm pure Al wire annealed at 300 °C for various times (data plotted in Fig. 7). From Table 4, we can see that the annealing of 1 mm pure Al wire (η=8.5) at 300 °C has no significant effect on its resistivity. This suggested that the resistivity contribution from increased dislocation density of pure Al wire due to deformation is negligible, and that the pure Al surface is quite resistant to oxidation to maintain its low resistivity. The surface of Al/Ca composite rapidly becomes essentially pure Al following exposure to air, so the composite wire should be resistant to oxidation as well.

From Table 3, we can see that the resistivity of Al/Ca (20 vol%) composite increases after annealing at 300 °C for 600 s. This resistivity increase is most likely attributed to intermetallic formation. Recall that Al_2Ca was observed to form at 275 °C in Al/Ca (9 vol%) composite (η=8.55) [6], and the DSC test on 1 mm Al/Ca (20 vol%) composite wire (η=8.5) suggested that Al_2Ca formed at 258.9 °C (see Fig. 5). To verify this, the resistivity of arc-melted pure Al_2Ca specimens (confirmed by X-ray diffraction) has been measured to be 0.1115 μΩ m,

Table 3
The electrical resistivities of 1 mm Al/Ca (20 vol%) composite wire (deformation true strain 8.5) annealed at 300 °C for different times.

Annealing time (s)	0	600	1200	1800	2400	3000	3600	4200	8400	9600	67,680
Electrical resistivity (10^{-4} μΩ m)	305	515	515	505	505	507	510	510	515	514	518

Table 4
The electrical resistivities of 1 mm pure Al wire (deformation true strain 8.5) annealed at 300 °C for different times.

Annealing time (s)	0	600	1200	1800	2400	3000	10,500	21,600	90,000
Electrical resistivity (10^{-4} μΩ m)	283	283	282	285	282	283	283	282	283

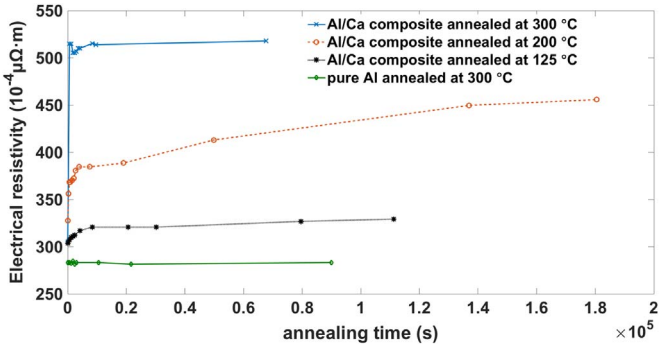

Fig. 7. Summary of the electrical resistivities of 1 mm dia. Al/Ca (20 vol%) composite wire as a function of annealing time at 300 °C, 200 °C, and 125 °C (data from Tables 3, 5, and 6 respectively), along with electrical resistivity data from 1 mm dia. pure Al wire (data from Table 4) annealed at 300 °C.

roughly 4 times that of pure Al. If we assume that all Ca filaments had been fully converted to Al_2Ca by annealing at 300 °C, the volume fraction for Al and Al_2Ca would be 40% and 60%, respectively. By using an inverse rule of mixtures, the resistivity of Al/Al_2Ca (60 vol%) composite is calculated to be 0.0513 μΩ m, which closely matches the measured resistivity value of 0.0515 μΩ m. This suggests that the initial resistivity increase due to annealing at 300 °C for only 10 min is caused by the complete transformation of Ca filaments into Al_2Ca.

To further understand the elevated temperature performance of Al/Ca composite wire, the resistivities were measured after annealing at 200 °C and 125 °C for various lengths of time, as shown in Tables 5 and 6 (data plotted in Fig. 7). Table 5 clearly shows that the resistivity increased after 10 mins annealing and then stabilized for another 25 mins. This could be due to the formation of intermetallic compound Al_4Ca, as one can see from the DSC curve in Fig. 4. Based on a simple inverse rule of mixtures (48 vol% Al and 52 vol% Al_4Ca) and the stable resistivity of Al/Ca wire at 25 mins, a resistivity of 0.0517 μΩ·m was derived for Al_4Ca. This is about half the value for Al_2Ca and twice the value of Al. After that, the resistivity of Al/Ca wire began to increase at a slow, nearly constant rate. This could be due to the slow decomposition of Al_4Ca to Al_2Ca at relatively low temperature (200 °C), since Al_4Ca is the less stable of the two compounds, as the DSC curves showed. Table 6 for annealing of the wire at 125 °C shows that the resistivity increased gradually up to 140 mins. This could result from the formation of Al_4Ca at 125 °C, but at a much slower rate than at 200 °C. If so, the Al_4Ca persisted for about 6 h, then began to decompose into Al_2Ca, as suggested by the slow resistivity rise in Fig. 7. It is worthwhile to mention that the 0 min resistivity result in Table 5 is somewhat different from those in Tables 3 and 6, probably due to some extra surface contamination during the resistivity sample preparation of Table 5. However, these surface impurities should not affect the resistivity increase during the isothermal annealing. To summarize, the formation of Al_4Ca and Al_2Ca seems to occur at all three temperatures with Al_2Ca being the more stable phase. As one would expect, the rate of formation and decomposition varies greatly with temperature.

From the equilibrium Al-Ca phase diagram [13], it is known that Al and Ca have essentially no mutual solid solubility at thermodynamic equilibrium. Al_2Ca formation may require a pre-existing Al/Ca solution, as suggested by the phase diagram and the fact that the pure Al_2Ca sample was obtained by arc melting to get a liquid solution of Al and Ca. Therefore, there is a possibility that the contact between pure solid Al and pure solid Ca would not form Al_2Ca at the interface because Al and Ca have no mutual solubility and would not form Al/Ca solid solution. In addition, the DSC results in Fig. 5 for the η=8.5 sample also suggests that the formation of the Al_2Ca was preceded by the formation of the Al_4Ca phase, presumably at the true Al/Ca interface where there is only slight penetration of the Ca atoms into the Al lattice, which make the Al_4Ca phase kinetically favored by this decreased interatomic mixing even though the driving force for formation of the Al_2Ca phase is higher.

However, there is a phenomenon called deformation-induced chemical mixing that has been widely observed in heavily co-deformed metallic composites [17]. This phenomenon can cause the complete dissolution of a minority filament phase into the matrix phase. Several mechanisms of deformation-induced mixing have been suggested. One such mechanism is dislocation shuffling, which suggests that the shear transfer by multiple slip systems of two phases across the heterophase interface can lead to massive chemical mixing by shearing tiny embedded one-phase particles into another phase. These tiny particles would dissolve into their surrounding phase through the curvature-driven, dissolution-Gibbs-Thomson effect due to the small size of particles, though the two phases are mutually insoluble under thermodynamic equilibrium.

This mechanism would seem to be applicable to some degree for the fcc Al and fcc Ca phases, since both share the same multiple slip systems. Table 3 presents one corroborating observation supporting this hypothesis because it shows that the resistivity after 10 min of annealing can be explained by the inverse rule of mixtures of pure Al (40 vol%) and pure Al_2Ca (60 vol%). This suggests occurrence of the eventual intermixing of Ca to form Al/Ca solid solution that eventually transforms into Al_2Ca during annealing. The DSC results in Fig. 5 also show that annealing above about 260 °C should also complete transformation to Al_2Ca at the Al/Ca interface. If Al_4Ca is formed by the initial reaction of Al and Ca at the interface, the diffusion barrier effect of Al_4Ca at the interface for transport of Al into Ca or Ca into Al should slow the kinetics of Al_2Ca formation substantially. This diffusion barrier effect does seem to be operating in this system since a higher temperature was needed to complete the transformation to Al_2Ca, although it is complete within 10 min of annealing at 300 °C. This

Table 5
The electrical resistivities of 1 mm Al/Ca (20 vol%) composite wire (deformation true strain 8.5) annealed at 200 °C for different times.

Annealing time (s)	0	300	600	900	1500	2100	2700	3900	7560	18,960	49,860	136,920	180,540
Electrical resistivity (10^{-4} μΩ m)	328	356	368	368	370	372	380	384	384	389	413	450	456

Table 6
The electrical resistivities of 1 mm Al/Ca (20 vol%) composite wire (deformation true strain 8.5) annealed at 125 °C for different times.

Annealing time (s)	0	600	1200	1800	2400	4200	8400	20,580	30,180	79,560	111,240
Electrical resistivity (10^{-4} μΩ m)	304	307	310	311	312	317	321	321	321	327	329

annealing temperature is higher than the onset of Al_2Ca formation at 260 °C that was observed on continuous heating in Fig. 5.

The observation (see Fig. 5) that a temperature as low as 177 °C is sufficient to start transforming the Al/Ca composite microstructure into an Al/intermetallic composite at even a modest deformation true strain of 8.5 has several implications. First, there might have to be a limit specified on the possible Joule heating that the conductor can tolerate, which would limit the range of possible applications for these conductors. Second, it is probably preferred that the whole deformation processing to the final level of deformation true strain should be completed in the Al/Ca composite state to prevent intermetallic transformation, so that all of the deformation above some significant level (maybe η=5) should be done at temperatures below about 150 °C. Of course, this deformation level limit and the processing temperature boundary must both be investigated experimentally to determine them with more precision. Third, it may be preferred to fully transform the Ca filamentary phase to an intermetallic phase, probably Al_2Ca after the completion of all desired deformation processing, to produce a conductor wire with the highest temperature stability and, effectively, to avoid having to place a limit on possible Joule heating from amperage overloads. This processing option also must be pursued in further work.

4. Conclusions

a) An Al/Ca (20 vol%) nanofilamentary composite was produced by powder metallurgy and severe plastic deformation, utilizing gas atomized fine Al powders and centrifugally atomized fine Ca powders.
b) After deformation processing, most Ca filaments adopted a ribbon-shaped morphology instead of the cylindrical morphology expected for fcc metal reinforcement filaments.
c) The strength of the composite increased with deformation true strain due to the strong interfacial strengthening from finer Ca filaments, which can be described well by a Hall-Petch barrier model.
d) An ultimate tensile strength of 476 MPa was achieved for the Al-Ca metal-metal composite, which is superior to currently available commercial aluminum conductors.
e) The resistivity of the composite was slightly higher than the inverse-rule-of-mixtures prediction presumably due to crystal defects such as oxide debris inclusions and dislocations.
f) Both DSC continuous heating tests and resistivity measurements after elevated temperature annealing suggested that the Al/Ca interfaces in the DMMC do transform to Al_4Ca and, subsequently, to Al_2Ca on heating.
g) The kinetics of initial Al_4Ca formation and Al_4Ca transformation into Al_2Ca are greatly enhanced at elevated deformation true strain values.

Acknowledgements

The authors appreciate the financial support of ISU's Electric Power Research Center, Iowa State University Research Foundation, U.S. Department of Energy Office of Electricity, and Summit Technology Group LLC. The authors appreciate Qingfeng Xing for focused ion beam and some scanning electron microscopy work, at Ames Laboratory's Sensitive Instrument Facility; Ryan Ott and Matt Besser for use of their Zwick/Roell Z2.5 tensile system; Charles Spellman of Psylotech for tensile testing the high eta Al/Ca specimens. The Ames Laboratory is operated for U.S. Department of Energy by Iowa State University contract no. DE-AC02-07CH11358.

References

[1] L. Tian, I. Anderson, T. Riedemann, A. Russell, H. Kim, Prospects for novel deformation processed Al/Ca composite conductors for overhead high voltage direct current (HVDC) power transmission, Electr. Power Syst. Res. 105 (2013) 105–114.
[2] A.M. Russell, L.S. Chumbley, Y. Tian, Deformation processed metal–metal composites, Adv. Eng. Mater. 2 (1–2) (2000) 11–22.
[3] J. Bevk, J.P. Harbison, J.L. Bell, Anomalous increase in strength of insitu formed Cu-Nb multifilamentary composites, J. Appl. Phys. 49 (12) (1978) 6031–6038.
[4] L. Tian, I. Anderson, T. Riedemann, A. Russell, Modeling the electrical resistivity of deformation processed metal–metal composites, Acta Mater. 77 (2014) 151–161.
[5] A.M. Russell, I.E. Anderson, H.J. Kim, A.E. Freichs, Aluminum/alkaline earth metal composites and method for producing, Google Pat. (2014).
[6] L. Tian, H. Kim, I. Anderson, A. Russell, The microstructure-strength relationship in a deformation processed Al–Ca composite, Mater. Sci. Eng.: A 570 (2013) 106–113.
[7] K. Xu, A.M. Russell, L.S. Chumbley, F.C. Laabs, V.B. Gantovnik, Y. Tian, Characterization of strength and microstructure in deformation processed Al-Mg composites, J. Mater. Sci. 34 (24) (1999) 5955–5959.
[8] A.M. Russell, T. Lund, L.S. Chumbley, F.A. Laabs, L.L. Keehner, J.L. Harringa, A high-strength, high-conductivity Al–Ti deformation processed metal matrix composite, Compos. Part A: Appl. Sci. Manuf. 30 (3) (1999) 239–247.
[9] L. Tian, Structure-property Relationships in an Al Matrix Ca Nanofilamentary Composite Conductor with Potential Application in High-voltage Power Transmission, Iowa State University, Ames, IA, 2015.
[10] J.R. Rieken, I.E. Anderson, M.J. Kramer, G.R. Odette, E. Stergar, E. Haney, Reactive gas atomization processing for Fe-based ODS alloys, J. Nucl. Mater. 428 (1–3) (2012) 65–75.
[11] O.D. Neikov, I. Murashova, N.A. Yefimov, S. Naboychenko, Handbook of Non-ferrous Metal Powders: Technologies and Applications, Elsevier, Amsterdam, The Netherlands, 2009.
[12] A.M. Russell, L.S. Chumbley, T.W. Ellis, F.C. Laabs, B. Norris, G.E. Donizetti, In situ strengthening of titanium with yttrium: texture analysis, J. Mater. Sci. 30 (17) (1995) 4249–4262.
[13] ASM-International, ASM Alloy Phase Diagram Database, Materials Park, OH, USA.
[14] C.A. Johnson, Generalization of the Gibbs-Thomson equation, Surf. Sci. 3 (5) (1965) 429–444.
[15] K. Ozturk, L.-Q. Chen, Z.-K. Liu, Thermodynamic assessment of the Al–Ca binary system using random solution and associate models, J. Alloy. Compd. 340 (1–2) (2002) 199–206.
[16] C. Kittel, Introduction to Solid State, John Wiley & Sons, 1966.
[17] D. Raabe, P.-P. Choi, Y. Li, A. Kostka, X. Sauvage, F. Lecouturier, K. Hono, R. Kirchheim, R. Pippan, D. Embury, Metallic composites processed via extreme deformation: toward the limits of strength in bulk materials, MRS Bull. 35 (12) (2010) 982–991.